Mesoscopic Junctions, Random Scattering, and Strange Repellers

M. L. Roukes and O. L. Alerhand
Bellcore, Red Bank, New Jersey 07701
(Received 15 May 1990)

Ballistic transport through a two-dimensional cross junction is chaotic. The classical transmissivity, from which total transmission coefficients are obtained, exhibits self-similar regions of high transparency about a hierarchy of injection angles, α_N. These *geometrical channels* dominate the phase space of possible exits from the junction. Long dwell times within the junction, a manifestation of irregular scattering, strongly enhance the role of random processes in real devices.

PACS numbers: 73.40.−c, 05.45.+b

Recently, anomalous magnetoresistance phenomena observed at "quantum wire" junctions have been successfully modeled by a remarkably simple *classical* model.[1] Closer comparison with experimental results, however, reveals significant differences which appear to arise from random scattering. These anomalies are fully manifested only when, with adequate mean free path and boundaries that are sufficiently reflective (i.e., *specular*), electrons can follow trajectories through junctions without loss of momentum memory.[2] Below, we quantify the requirements of the classical model by determining precisely how "specular" and how "ballistic" transport must be before fully developed anomalies emerge. This exploration unveils the intrinsically chaotic nature of electron transport through a two-dimensional (2D) cross junction.

The devices used in experiments are here modeled by infinite-wall potentials forming the edges of a symmetric 2D junction.[3] Junction geometry is completely specified by a single parameter $\hat{r}=r_J/W$, where r_J is the (constant) radius of curvature of the corners and W is the width of the probes leading to the junction. (Carets denote lengths normalized to W.) The transition from $\hat{r}=0$ to values $\gg 1$ describes a smooth evolution from a square- to a round-cornered junction [Fig. 1(a), insets]. We calculate classical transmission coefficients T_{ij} (the total fraction of flux injected via lead j which emerges in lead i) by integrating classical trajectories over the incident (y_j,α_j) and outgoing (y_i,α_i) phase spaces of the probes:

$$T_{ij}=\int dy_i\, d\alpha_i\, dy_j\, d\alpha_j\, g(y_j,\alpha_j)\, T_{ij}(y_i,\alpha_i|y_j,\alpha_j)\,. \quad (1)$$

Here, y_j and α_j are the transverse coordinate and angular direction of a particle at the boundary between lead j and the junction proper.[4] The *classical transmissivity* $T_{ij}(y_i,\alpha_i|y_j,\alpha_j)$, appearing as the kernel of Eq. (1), is the amplitude (either 0 or 1) that a trajectory exists linking specific coordinates in the incident (y_j,α_j) and outgoing (y_i,α_i) spaces. Equation (1) is weighted by the incident electron distribution function $g(y_j,\alpha_j)$. At $B=0$, for infinite-wall potentials and the simplest connection to electron reservoirs, $g(y_j,\alpha_j)=\cos(\alpha_j)/2W$. These simplifications reduce the problem to that of classical billiards: T_{ij} are calculated following trajectories of (typically 10^5) electrons as they traverse the junction. Subsequently, Büttiker's model[5] provides a prescription for calculating resistances from the T_{ij} obtained.

Figure 1(a) shows the dependence of the transmission probabilities upon junction geometry. Exact results obtained analytically for $\hat{r}=0$ ($T_F=\sqrt{2}-1$, $T_S=1-\sqrt{2}/2$, $T_B=0$), smoothly evolve to asymptotic values ($T_F=T_S=T_B=\frac{1}{4}$) as $\hat{r}\to\infty$. Solid lines in Figs. 1(a) and 1(b) display results for the idealized case where, as in Ref. 1, it is assumed that the mean free path l_0 is infinite and reflections at the boundaries are completely specular. (The dashed lines, discussed below, display the effect of random scattering.) The trend toward asymptotic equalization of the T_{ij} occurs through *scrambling*[1]—after injection into a rounded junction electrons bounce many times before finding an exit port. This trend emerges for $\hat{r}>1$ when the width of the exits, $W\equiv 1$, becomes small compared to the extent of the junction itself, $\hat{l}=2\hat{r}+1$. Interestingly, T_F remains *flat* up to $\hat{r}\sim 3$, beyond which it is reduced by scrambling. This behavior apparently contradicts the conjectured importance of *collimation*,[6,7] which is supposed to enhance T_F when, with increasing $\hat{r}$, the leads become increasingly flared at the junction. We discuss this below.

The negative bend resistance[8] at zero magnetic field, $R_B(0)=(T_S-T_F)/[4T_S(T_S+T_F)]$, elucidates the interplay between T_{ij}. Figure 1(b) shows that $R_B(0)$, normalized to the classical ballistic lead resistance $R_0=(\hbar\pi/e)^2(1/p_FW)$, starts from its exact value at $\hat{r}=0$, $(1/\sqrt{2}-\frac{3}{4})/(1-1/\sqrt{2})\sim -0.146$, and vanishes as $\hat{r}\to\infty$ due to asymptotic equalization. A pronounced dip occurs near $\hat{r}\sim 3$ because T_S decreases while T_F remains roughly constant. This decrease in T_S, and the enhancement of $|R_B|$, are strongest at $\hat{r}_{\rm crit}=1+\sqrt{2}$ when direct paths from the injection lead to the side leads are "shadowed" by rounded corners.

Figures 1(c) and 1(d) quantify what is required for the simple model to hold. Figure 1(c) shows the average number of boundary reflections, $\langle N_{ij}\rangle$, suffered while passing from lead j to each exit lead, i. Similarly, Fig. 1(d) shows the average path length $\langle \hat{S}_{ij}\rangle$ traversed. Both rise dramatically beyond $\hat{r}\sim 1$. Fine dotted lines denote the regime of a recent experimental test of the classical model.[2] In these experiments, memory loss is estimated to occur, on average, after ~ 7 boundary collisions.[9(b)] Figure 1(c) shows that $\langle N_{ij}\rangle\sim 7$ for $\hat{r}\sim 3$. The mean free path, which decreases when electron density is re-

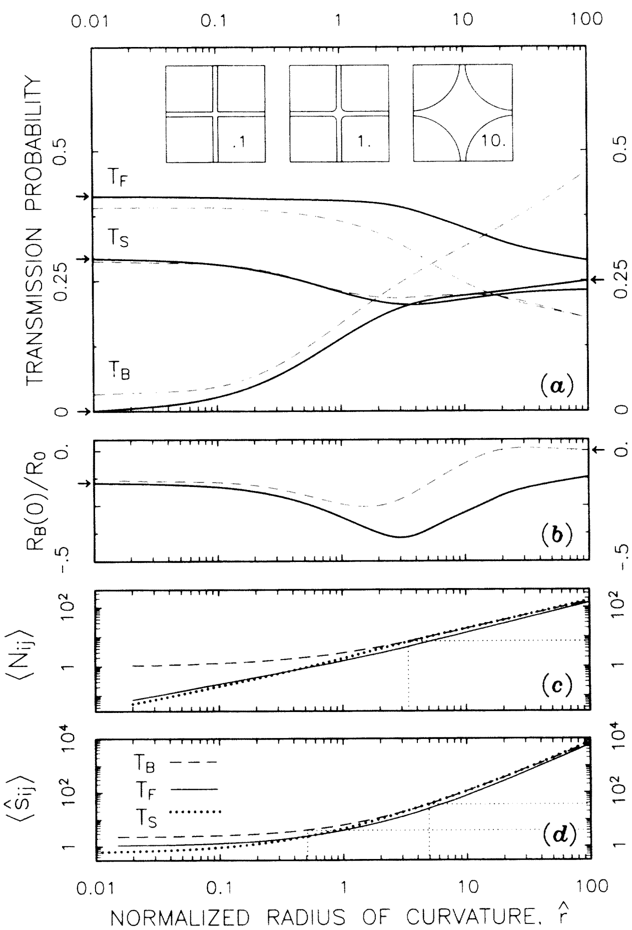

FIG. 1. Summary of the simple model. (a) Transmission probabilities for forward (T_F), side (T_S), and backscattering (T_B), as a function of junction geometry (solid lines). Arrows at left show analytic results for $\hat{r}=0$. Top insets: Junctions for three values of $\hat{r}$. (b) Solid line shows the $B=0$ bend resistance, proportional to T_S-T_F. Enhancement at $\hat{r}\sim 3$ arises from "shadowing," but scrambling suppresses $R_B(0)\rightarrow 0$ as $\hat{r}\rightarrow\infty$. *Dashed lines in (a) and (b) show the effect of random scattering (see text).* (c),(d) Average number of boundary reflections $\langle N_{ij}\rangle$ and average path length traversed $\langle \hat{S}_{ij}\rangle$ in passing through the junction to each exit lead.

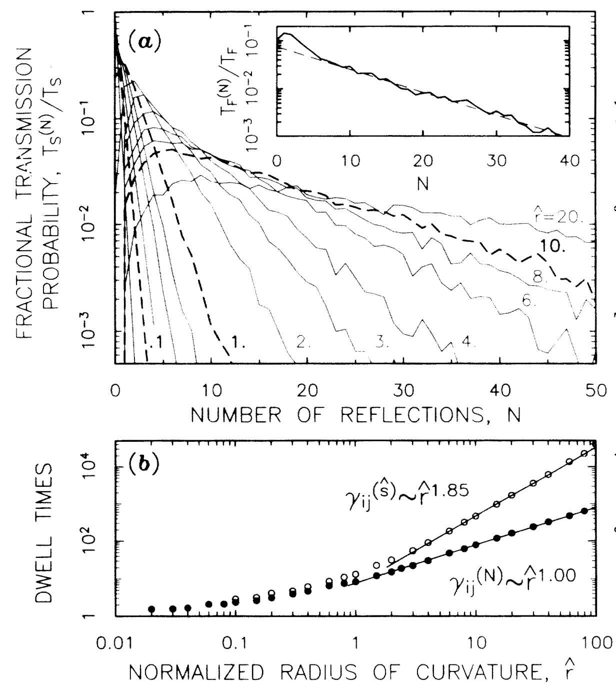

FIG. 2. Statistics of junction transmission. (a) The fractional weight of terms in T_S involving exactly N reflections, for a family of $\hat{r}$ values. (b) Dwell times vs geometry for the N- and $\hat{S}$-fractional distributions. In both cases all leads show identical behavior.

duced,[2] varied from $\hat{l}_0\sim 36$ to $\hat{l}_0\sim 4$.[10] Accordingly, Fig. 1(d) shows that $\langle \hat{S}_{ij}\rangle$ attains these values for $\hat{r}\sim 5$ and 0.5, respectively. Note that these *average* values, $\langle N_{ij}\rangle$ and $\langle \hat{S}_{ij}\rangle$, verge on what is experimentally available *even for moderate* $\hat{r}$, showing that scattering significantly affects T_{ij} over the entire regime of recent experiments.

In the presence of random scattering we picture the transmission probabilities as comprising both deterministic and random parts: $T_{ij}=T_{ij}^{(\mathrm{det})}+T_{ij}^{(\mathrm{ran})}$. An electron scattered from its initial (deterministic) trajectory may ultimately exit through *any* lead. Naively, we might assume it then contributes equally to the $T_{ij}^{(\mathrm{ran})}$. Without further refinements, the idealized model can be employed to determine the relative weight of $T_{ij}^{(\mathrm{det})}$ and $T_{ij}^{(\mathrm{ran})}$ in real samples. We calculate the *fractional* transmission probabilities for each exit lead i, $T_{ij}^{(N)}/T_{ij}$ and $T_{ij}^{(\hat{S})}/T_{ij}$, formed solely from trajectories involving exactly N reflections or requiring traversal of exactly $\hat{S}$ units of path length, respectively. For brevity we show only one of these, $T_S^{(N)}/T_S$, for transmission into a side probe [Fig. 2(a)]. Its behavior is generic to all: For small $\hat{r}$ a peak at low N is followed by a strict exponential decay. As $\hat{r}$ increases, low-N terms become precipitously suppressed. For $\hat{r}>1$ there is a rapid increase in the exponential decrements, which we term *dwell times*,[11] $\gamma_{ij}^{(\hat{S})}$ and $\gamma_{ij}^{(N)}$. (These are extracted from the fractional distributions [see Fig. 2(a), inset].) Their steep rise quantifies the dramatically increasing weight of high-order terms. On a linear scale the distributions ultimately become almost flat; averages [Figs. 1(c) and 1(d)] have little meaning. This behavior signifies that, even for moderate $\hat{r}$, many electrons become temporarily trapped, following complicated trajectories before leaving the junction. *This increase in the γ_{ij}'s presages the emergence of fully chaotic behavior in $T_{ij}(y_i,\alpha_i|y_j,\alpha_j)$.*

The irregular nature of 2D junction scattering is clearly evident in Fig. 3(a), where we plot

$$N_F(y_j,\alpha_j)=N(y_j,\alpha_j)\Big/\int dy_F\,d\alpha_F\,T_F(y_F,\alpha_F|y_j,\alpha_j)$$

vs α_j, for $y_j=0$, where $N(y_j,\alpha_j)$ is the number of reflections sustained in transversal, beginning from (y_j,α_j). Simply stated, N_F displays the number of reflections required for junction traversal, for those α_j

which ultimately lead into the forward probe. Two distinct features are exhibited. First, we mark by arrows a sequence of finite angular apertures, *geometrical channels,* comprising direct exit paths. Second, outside of these apertures the transmissivity appears erratic. We discuss these in turn.

The geometrical channels are finite regions of incident phase space leading to short exit paths and few reflections within the junction. In real samples, these collections of trajectories are least susceptible to random scattering and provide the principal contribution to $T_{ij}^{(\mathrm{det})}$. We denote the angular positions and apertures of the principal channels by α_N and $\Delta\alpha_N$, respectively. The central channel, for example, is a cone of trajectories leading *directly* ($N=0$) into the forward lead: $\alpha_0=0$ and $\Delta\alpha_0=2\tan^{-1}[1/2(2\hat{r}+1)]$. For the case of T_F, low-N principal channels constitute the vestiges of collimation in a cross junction. (Viewed strictly, the concept of collimation pertains directly only to a simple horn geometry.[6]) Contributions from collimated electrons appear as a small rise at low N upon a large, exponentially decreasing background dominated by irregular scattering, i.e., *scrambling* [Fig. 2(a), inset].

Self-similarity, characteristic of chaotic dynamics,[12] is evident in Fig. 3(b), where the first eight principal channels are separately magnified. Their sequence of positions $\{\alpha_N\}$ and apertures $\{\Delta\alpha_N\}$ satisfy simple asymptotic scaling relations: $\lim_{N\to\infty}\Delta\alpha_N/\Delta\alpha_{N-1}=f(\hat{r})$ and $\lim_{N\to\infty}(\alpha_{N+1}-\alpha_N)/(\alpha_N-\alpha_{N-1})=f(\hat{r})$. We also find exact expressions, valid for all N:

$$\alpha_N=\frac{\pi}{2}\frac{1-f(\hat{r})^N}{1+f(\hat{r})^N}\,,\quad \Delta\alpha_N=2\Delta\alpha_0\frac{f(\hat{r})^N}{1+f(\hat{r})^N}\,. \tag{2}$$

Through such relations, the function $f(\hat{r})$ generates the complete structure of phase space. (For our model, $f(\hat{r})\approx\exp[(2/\hat{r})^{1/2}]$.) Within each channel a staircase of higher plateaus appears. These scale similarly, and occur when the number of reflections in the collection lead progressively increases by 1. Equations (2) are specific to our simple model, but we expect that the self-similarity demonstrated is generic to irregular junction scattering in 2D. Although our brief discussion pertains only to injection on axis ($y_j=0$), the entire phase space is organized in self-similar fashion (Fig. 4).

Outside of the principal channels the transmissivity appears to depend erratically upon injection angle α_j. Electrons injected *outside* $\{\alpha_N\}$ generally suffer many reflections before emerging; this leads to large γ_{ij} [Fig. 2(b)]. This is one manifestation of the *strange repeller*—the set of closed orbits within the junction—which is at the heart of the chaotic behavior. These closed orbits are not accessible from the incident (y_j,α_j) phase space. However, if an injected electron closely approaches such an orbit after several reflections, it can persist in a quasistable trajectory until it is finally expelled from the junction. (In the limit $\hat{S}\to\infty$, $\gamma_{ij}^{(S)}$ give a measure of the fractal dimension of the repeller.[12])

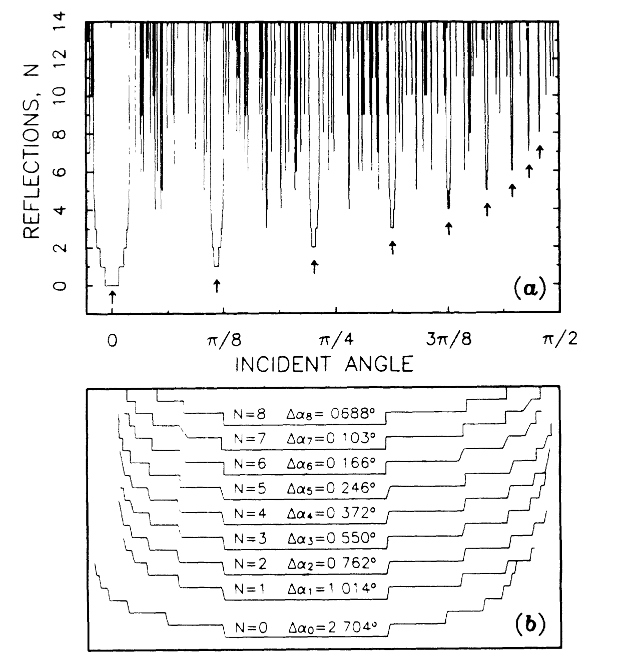

FIG. 3. Geometrical channels of T_F, for $\hat{r}=10$. (a) Number of boundary reflections N vs incident angle α_j for electrons injected on axis and collected in the forward lead. Arrows mark principal geometrical channels, α_N. These are separately magnified in (b) to display their self-similarity; their respective angular apertures are noted.

Another striking property of the repeller is its fractal organization of phase space. Two electrons injected with arbitrarily close coordinates in (y_j,α_j), yet outside the apertures $\{\Delta\alpha_N\}$, will follow trajectories differing arbitrarily in the number of reflections sustained. *In general, this pair of electrons will not emerge from the junction via the same lead.*[9(a)] (By contrast, all electrons within a given $\Delta\alpha_N$ follow the *same* sequence of reflections.) The seemingly random regions of phase space outside $\{\Delta\alpha_N\}$ are actually completely structured into successive, self-similar hierarchies of higher-order trajectories.

Figure 4(a) shows the evolution of the map of angles $\alpha_j^{(F)}$ representing electrons injected on axis ($y_i=0$) and collected into the forward lead, as a function of $\hat{r}$. Dark bands correspond to principal geometric channels $\{\Delta\alpha_N\}$; higher-order channels split off from these as finer bands. As $\hat{r}$ increases, the measure of phase space occupied by the principal set $\{\alpha_N\}$ diminishes—asymptotically the T_{ij} become equalized. A complete map of the 2D phase space of electrons collected into the forward lead ($y_j^{(F)}$, $\alpha_j^{(F)}$) is shown in Fig. 4(b) for $\hat{r}=5$.

Principal geometrical channels $\{\alpha_N\}$ provide the largest contribution to $T_{ij}^{(\mathrm{det})}$ for each exit lead i. As N increases, however, fewer electrons survive random scattering while traversing what become increasingly more complicated paths through the junction. We explore this, modeling diffuse boundaries by ascribing a probability p that electrons reflect specularly and a probability $1-p$ that they scatter randomly after each boundary col-

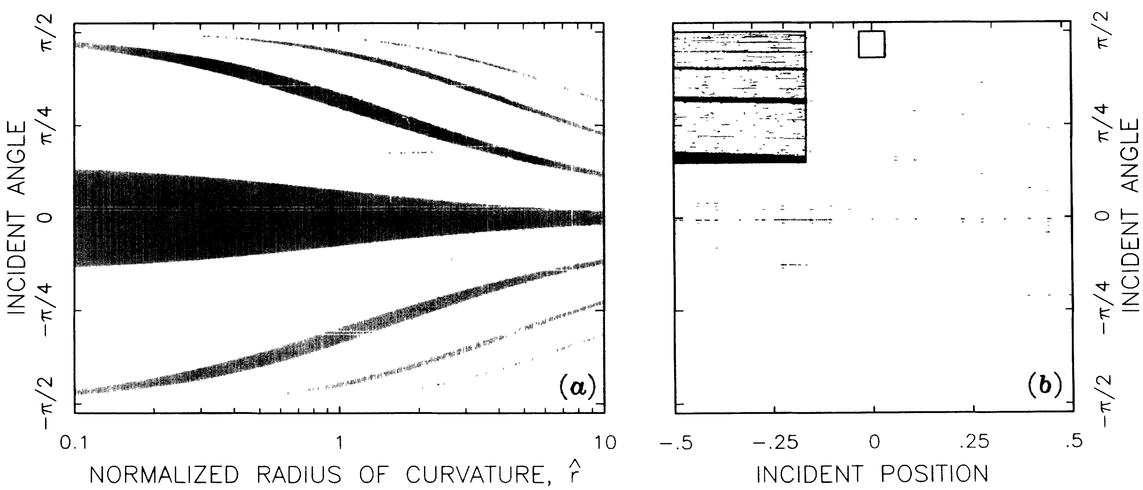

FIG. 4. Fractal nature of 2D junction transmissivity. (a) Map of incident angles $\alpha_j^{(F)}$ for electrons injected on axis and collected into the forward lead vs $\hat{r}$. Principal geometrical channels $\{\alpha_N\}$ appear as dark bands. (b) Map of incident coordinates $(y_j^{(F)},\alpha_j^{(F)})$ of electrons collected into the forward lead for a junction with $\hat{r}=5$. Upper-left inset: Blowup of region in the smaller box at the top center. Complementary maps of electrons collected into other leads (*not shown*), $(y_j^{(S)},\alpha_j^{(S)})$ and $(y_j^{(B)},\alpha_j^{(B)})$, exhibit similar characteristics.

lision.[13] This introduces a *transparency* of p^N to the Nth geometrical channel. Finite mean free paths are modeled by introducing a probability $1-\exp(-\hat{l}/\hat{l}_0)$ that an electron scatters elastically (with angular isotropy) within the junction's interior. Here $\hat{l}$ is the distance traveled since the previous scattering event. The effect of such random scattering upon the T_{ij} and upon $R_B(0)$, for values $p=0.88$ and $\hat{l}_0=20$ chosen to approximate the regime of Ref. 2, are shown in Figs. 1(a) and 1(b) as dashed lines. Even within these simple approximations memory-loss scattering does not occur isotropically within the junction; $T_{ij}^{(\mathrm{ran})}$ contribute *unequally* to each exit lead i [Fig. 1(a)]. The net effect of random processes is to eliminate contributions to $T_{ij}^{(\mathrm{det})}$ from trajectories involving large N and large $\hat{S}$. As a result, transport anomalies, such as $R_B(0)$, become completely suppressed with only moderate junction rounding—well before deterministic scrambling becomes manifest [Fig. 1(b)].

We have described the chaotic nature of the classical transmissivity $T_{ij}(\alpha_i,y_i|\alpha_j,y_j)$ in a 2D cross junction.[14] Even after integration to yield transmission coefficients, a strong signature of irregular dynamics persists. We find the fractal nature of phase space in a rounded junction enhances the role of random scattering, resulting in the premature suppression of transport anomalies. Note that recent experiments involve ballistic, *quasi-one-dimensional*, junctions. In these, transport involves only several modes and the occupation number is variable through a gate potential.[2] The fractal behavior emerging in this work, however, involves *continuous* phase-space coordinates. This suggests future explorations in multimode junctions where a transition from classical to quantized irregular transport might be observed.

We thank C. W. J. Beenakker, J. P. Crutchfield, and J. P. Heritage for helpful discussions.

[1]C. W. J. Beenakker and H. van Houten, Phys. Rev. Lett. **63**, 1857 (1989).

[2]M. L. Roukes, A. Scherer, and B. P. Van der Gaag, Phys. Rev. Lett. **64**, 1154 (1990).

[3]At sample edges strong variation in density occurs over a depletion length l_d [Ref. 9(b)]. Our model is most appropriate for samples where $l_d \sim 2\pi/k_F \ll W$ [see, e.g., A. Scherer and M. L. Roukes, Appl. Phys. Lett. **55**, 377 (1989), and Ref. 2].

[4]Only angular *direction* α_j appears—we assume all electrons have velocity v_F.

[5]M. Büttiker, Phys. Rev. Lett. **57**, 1761 (1986).

[6]C. W. J. Beenakker and H. van Houten, Phys. Rev. B **39**, 10445 (1989).

[7]H. U. Baranger and A. D. Stone, Phys. Rev. Lett. **63**, 414 (1989).

[8]Y. Takagaki *et al.*, Solid State Commun. **68**, 1051 (1988).

[9](a) C. W. J. Beenakker and H. van Houten, in *Electronic Properties of Multilayers and Low-Dimensional Semiconductor Structures*, edited by J. M. Chamberlain, L. Eaves, and J. C. Portal (Plenum, London, 1990); (b) M. L. Roukes *et al.*, *ibid.*

[10]In the experiments of Ref. 2, l_0 decreased from 9 to <1 μm as density was reduced. Since $W \sim 0.25$ μm, $\hat{l}_0 \sim 36$ and ~ 4, respectively.

[11]The $\gamma_{ij}^{(\hat{S})}$ represent dwell *times* if multiplied by the transit time, $\tau_T = W/v_F$ (~ 1 ps for Ref. 2).

[12]B. Eckhart, J. Phys. A **20**, 5971 (1987); U. Smilansky, in *Chaos and Quantum Physics*, edited by M.-J. Giannoni, A. Voros, and J. Zinn-Justin (Elsevier, New York, 1990).

[13]K. Fuchs, Proc. Cambridge Philos. Soc. **34**, 100 (1938).

[14]Advances in "electron optics" in a 2DEG should permit injection of a 2D "beam" by placing angular and spatial collimators after a point contact. For this case, $g(y_j,\alpha_j) \sim \delta(y_j)\delta(\alpha_j)$, and the $\{\alpha_N\}$ should become directly observable.

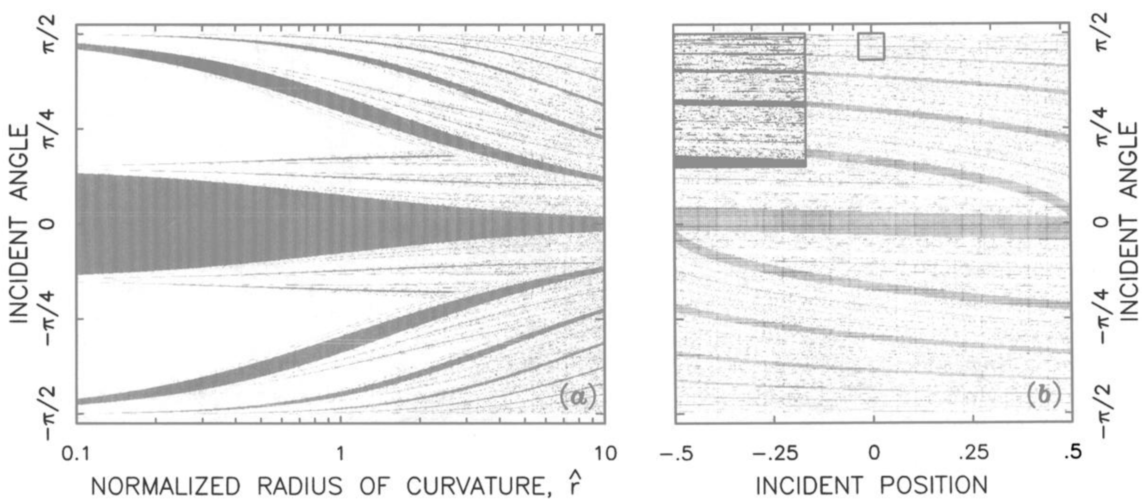

FIG. 4. Fractal nature of 2D junction transmissivity. (a) Map of incident angles $\alpha_j^{(F)}$ for electrons injected on axis and collected into the forward lead vs $\hat{r}$. Principal geometrical channels $\{\alpha_N\}$ appear as dark bands. (b) Map of incident coordinates $(y_j^{(F)},\alpha_j^{(F)})$ of electrons collected into the forward lead for a junction with $\hat{r}=5$. Upper-left inset: Blowup of region in the smaller box at the top center. Complementary maps of electrons collected into other leads (*not shown*), $(y_j^{(S)},\alpha_j^{(S)})$ and $(y_j^{(B)},\alpha_j^{(B)})$, exhibit similar characteristics.